COBALT-CATALYSED SYNTHESIS OF HYDROCARBON CO/H_2, STUDIED WITH TRANSIENT KINETICS (Task 3)

Chapter 1.0

INTRODUCTION

For a single, unidirectional step, the Turn-Over-Frequency (TOF), defined as reaction rate per surface-exposed atom, is related to the reactivity (k, s^{-1}) and the abundance (θ) of reaction intermediates as follows:

$$TOF = k \times \theta \qquad (1.1)$$

Considerable information[1-8]* has been obtained regarding the value of k and θ in methanation. However, the information about the values of k and θ for higher hydrocarbons in the Fischer-Tropsch (FT) synthesis is scanty.

With various techniques, e.g., IR, isotope transient response, consistent results[1-10] were obtained regarding the low surface coverage in growing chains. In these investigations a C_1-building block for the chain-growth in

*Parenthetical references placed superior to the line of text refer to the bibliography

**Page numbers in the upper right hand corner of this and succeeding pages refers to the page number in the thesis represented by this section.

Fischer-Tropsch Synthesis which does not contain oxygen (i.e., CH_x with probably x=2) has been suggested. In the production of higher hydrocarbons, Biloen and coworkers[4-6] have suggested one single pool of C_1 intermediates from which both methane and higher hydrocarbons are produced. However, there is not enough evidence for this suggestion and further investigation is needed to substantiate this proposal.

This work was undertaken with the objective to learn more about the origin of the effects reported recently[9] for introduction of ThO_2 and H-ZSM5 in the Co-based Fischer-Tropsch system. According to our workplan we completed in the first year work on the cobalt system itself. A full account of this work is being given in the next sections.

CHAPTER 2.0
INFORMATION FROM ISOTOPIC TRANSIENTS

2.1 GENERAL CONSIDERATION

For the convenience of the analysis of the experimental results, a hypothetic mechanism of the FT synthesis is presented in Fig.2-1.

CO is first adsorbed on the exposed surface. This adsorbed CO has a lifetime τ_0 before it changes to a C_1 surface intermediate or desorbs to CO in the gas phase. The C_1 surface intermediate then either terminate to produce CH_4 in the gas phase or react with a C_1-building surface intermediate to form C_2 surface intermediates. The C_1 surface intermediate has a lifetime τ_1, whereas the C_1-building intermediate has a lifetime τ_b. This model assumes the same propagation for C_2 and C_3 surface intermediates. They all propagate via the C_1-building surface intermediates. Their lifetimes are τ_2 and τ_3, respectively.

Let us consider an arbitrary area of the catalyst surface, containing N_s surface-exposed catalyst atoms (Fig.2-1). At the steady state this surface is covered with a pool of ^0N CO surface intermediates, a pool of ^1N C_1 surface intermediates, a pool of ^2N C_2 surface intermediates, etc. The inlet to pool C_1 is ^1R (defined as the number of

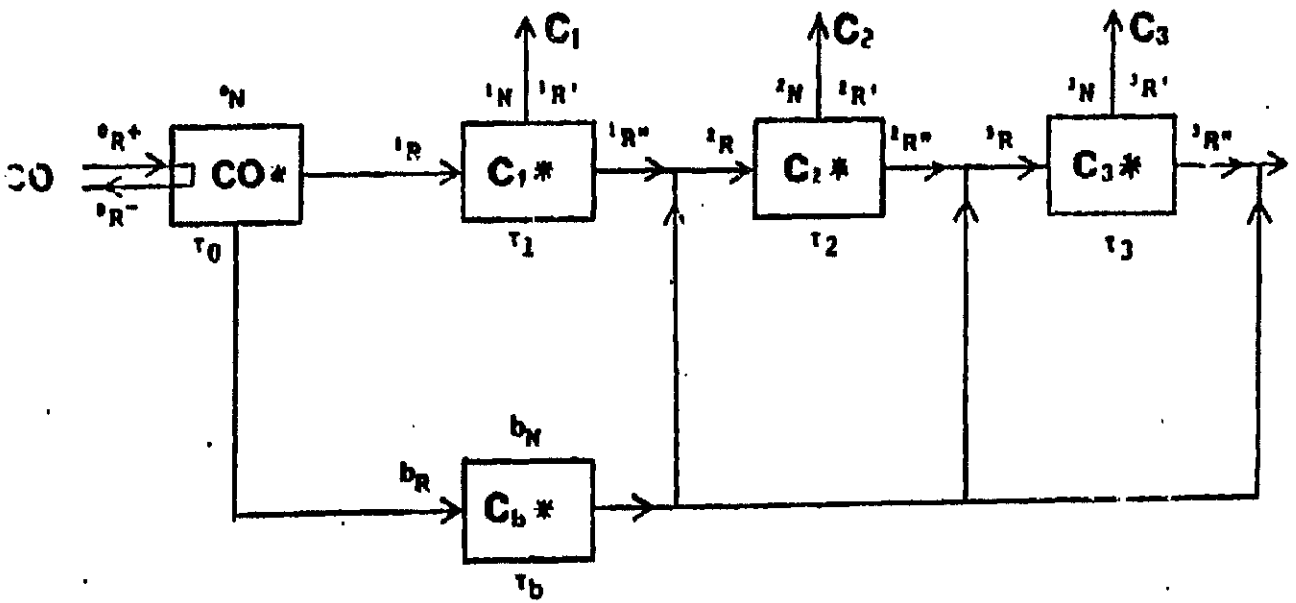

Figure 2-1: A hypothetic Mechanism of the FT synthesis

CH_x per second), to pool C_2 is ^2R, etc. In the following two sections we will define some terms and make several assumptions.

2.2 DEFINITIONS

2.2.1 The Reaction Rate

Fig.2-2 shows an arbitrary pool containing C_k surface intermediates.

^kR is the rate of inlet to pool C_k defined as the number of C_kH_y per second.

There are two outlets from pool C_k. One leads to the product, whereas the other leads to the surface intermediate.

In other words, $^kR'$ is the rate of formation of C_k products (in the gas phase) produced from pool C_k. $^kR''$ is the rate of formation of intermediate C_{k+1} produced from pool C_k.

Apparently,

$$^kR = {}^kR' + {}^kR'' \qquad (2\text{-}1)$$

Notice that among ^kR, $^kR'$ and $^kR''$ only $^kR'$ is observable. A further assumption regarding the relation between ^kR, $^kR'$ and $^kR''$ will be made in Section 2.3.

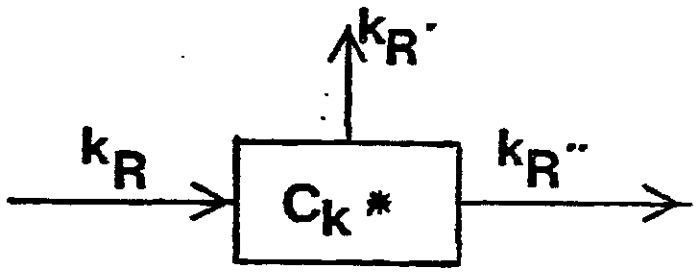

Figure 2-2: An arbitrary pool containing C_k intermediates

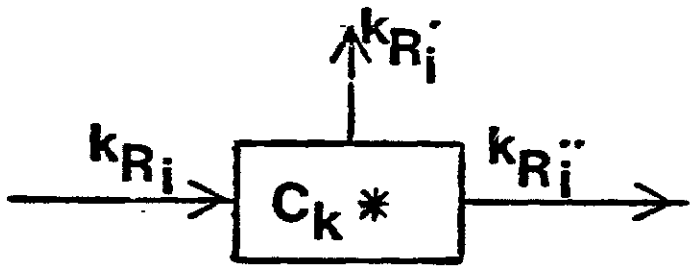

Figure 2-3: The reaction rate of species i and pool C_k

To form a C_{k+1} one C_k from pool C_k and one C_b is needed. Therefore,

$$b_R = \sum_{R=1}^{\infty} k_{R''} \qquad (2\text{-}2)$$

and

$$k_{R''} = {}^{k+1}l_R \qquad (2\text{-}3)$$

2.2.2 Isotopic Species of C_k

After we switch from ^{12}CO to ^{13}CO, the outlet from a pool will contain molecules with ^{12}C only, molecules with ^{13}C only, and molecules with both ^{12}C and ^{13}C. Since they are from the same pool, the number of carbon atoms in these molecules is the same. For example, from pool C_2, the following isotopic species are possible: $^{12}C_2H_4$, $^{12}C_1{}^{13}C_1H_4$, and $^{13}C_2H_4$.

In order to make writing easier, we use the word "species i" to represent molecules with constitution $^{12}C_i{}^{13}C_{k-i}$. For instance, in the C_2 case, species i represents one of the forms among $^{12}C_2H_4$, $^{12}C_1{}^{13}C_1H_4$, and $^{13}C_2H_4$.

2.2.3 The Rate of Species i from Pool C_k

Fig.2-3 shows an arbitrary pool containing C_k surface intermediates. ${}^{k}R_i$ is the rate at which species i enters to pool C_k.

There are two outlets from pool C_k. One is product, whereas another is a surface intermediate. Therefore, ${}^{k}R_i'$ is the rate of formation of species i (in the gas phase) from pool C_k. and ${}^{k}R_i''$ is the rate of production of species i intermediates from pool C_k.

Notice that among ${}^{k}R_i$, ${}^{k}R_i'$ and ${}^{k}R_i''$ only ${}^{k}R_i'$ is observable. An assumption on the relation between ${}^{k}R_i$, ${}^{k}R_i'$, and ${}^{k}R_i''$ has been made in Section 2.3 in order to enable mathematical treatment.

A distinction between ${}^{k}R$ and ${}^{k}R_i$ is very important. ${}^{k}R$ is the rate of entrance of all isotopic species into pool C_k while ${}^{k}R_i$ is the rate of of entrance of only one istopic species. For instance, in the C_2 case,

$$ {}^{2}R = {}^{2}R_{1,2}C_2H_4 + {}^{2}R_{1,2}C_1{}^{1,3}C_1H_4 + {}^{2}R_{1,3}C_2H_4 \qquad (2\text{-}4) $$

In general, for pool C_k:

$$ {}^{k}R = \sum_{i=0}^{n} {}^{k}R_i \qquad (2\text{-}5) $$

The similar relations are held for ${}^{k}R'$ and ${}^{k}R_i'$, and ${}^{k}R''$ and ${}^{k}R_i''$:

$$k_{R'} = \sum_{i=0}^{n} k_{R'_i} \qquad (2\text{-}6)$$

$$k_{R''} = \sum_{i=0}^{n} k_{R''_i} \qquad (2\text{-}7)$$

2.2.4 Transient Response of Species i

Defining:

k_{N_i} ≡ number of surface intermediates with constitution $^{12}C_i{}^{13}C_{k-i}$.

k_N ≡ number of surface intermediates in pool C_k.

k_{F_i} is the fraction of all C_k species with isotopic constitution $^{12}C_i{}^{13}C_{k-i}$:

$$k_{F_i} \equiv k_{N_i} / k_N \qquad (2\text{-}8)$$

2.2.5 Transient Response of ^{13}C and ^{12}C in the Outlet from a Pool

^{13}C and ^{12}C are contained in various species, say, in $^{13}C_2$ and $^{13}C_1{}^{12}C_1$.

We Define:

$F_{^{13}C \text{ in } C_k}$ ≡ (Number of ^{13}C atoms in pool C_k) / (Total number of C atoms in pool C_k)

$F_{^{12}C_k}$ ≡ (Number of ^{12}C atoms in pool C_k) / (Total number of C atoms in pool C_k)

It then follows that:

$$F^{13}C \text{ in } C_2 = {}^2F^{13}C_2 + 1/2\,{}^2F^{13}C_1{}^{12}C_1 \qquad (2\text{-}9)$$

$$F^{12}C \text{ in } C_2 = {}^2F^{12}C_2 + 1/2\,{}^2F^{13}C_1{}^{12}C_1 \qquad (2\text{-}10)$$

$$F^{13}C \text{ in } C_3 = {}^3F^{13}C_3 + 2/3\,{}^3F^{13}C_2{}^{12}C_1 + 1/3\,{}^3F^{13}C_1{}^{12}C_2 \qquad (2\text{-}11)$$

and

$$F^{12}C \text{ in } C_3 = {}^3F^{12}C_3 + 2/3\,{}^3F^{12}C_2{}^{13}C_1 + 1/3\,{}^3F^{12}C_1{}^{13}C_2 \qquad (2\text{-}12)$$

The coefficients (1/2, 1/3, 2/3, etc) are determined by the following expression:

For ^{12}C, coefficient = i / k.

For ^{13}C, coefficient = (k-i) / k.

For instance, in C_2, total carbon number, k, is 2, and ^{13}C number in $^{13}C_1{}^{12}C_1$ is 1. Therefore, Coefficient = 1/2.

2.2.6 Carbon Building Pool

It is impossible for our instrument to observe the transient response of C_1-building surface intermediates, since it only appears on the catalyst surface. Therefore, the transient response of the C_1- building pool. cannot be observed straightforwardly.

Further to Fig.2-1, we have:

1. ^{b}R is the rate of inlet to pool C_b.

2. $^{b}R{:}^{12}C$ is the rate of outlet of ^{12}C from pool C_b.

3. $^{b}R{:}^{13}C$ is the rate of outlet of ^{13}C from pool C_b.

4. The transient response is defined as:

$$^{b}F{:}^{12}C \equiv {}^{b}N{:}^{12}C/{}^{b}N \qquad (2\text{-}13)$$

$$^{b}F{:}^{13}C \equiv {}^{b}N{:}^{13}C/{}^{b}N \qquad (2\text{-}14)$$

2.3 ASSUMPTIONS

1. With the exception of CO chemisorption, the surface reaction are undirectional, as shown in Fig. 2-1.

2. There is no isotopic effect on reaction rate. With this assumption, the denominator in the definition of $^{k}F_i$ is constant, i.e., ^{k}N = constant. Therefore, $\sum_{i=0}^{k} {}^{k}F{:}^{13}C_i \, {}^{13}C_{k-i} = 1$.

   Notice that the absence of isotopic effect does not require the surface to be homogeneous.

3. Homogeneous surface: all surface species bearing the same label (e.g., $^{12}C_i{}^{13}C_{k-i}$) behave identical. Therefore, with the definition of $^{k}F_i$ (Eq.2-8, section 2.2.4), we have:

$$^{k}R_i'/^{k}R' = {}^{k}R_i''/^{k}R'' = {}^{k}F_i \qquad (2\text{-}15)$$

With the above assumptions, the pools will behave as the surface CSTR's, i.e., Continuous Stirring Tank Reactors.

Based on the above assumptions, we shall theoretically derive general equations for the transient response of species i. Then we will attempt to develop some criteria in order to answer the following questions:

1. Is the lifetime for the C_1-building intermediate very short compared with the C_1 intermediate?

2. Is the lifetime for the C_2 intermediate observable?

3. Is the lifetime for the C_3 intermediate observable?

We will start with $^{2}F_{1,3}C_1{}^{12}C_1$ to answer the first two questions. Then we will discuss the relation between $F_{1,3}C$

in C_3, $F^{13}C$ in C_2 and $^1F^{13}C_1$. A switch from ^{12}CO to ^{13}CO is assumed throughout the discussion.

2.4 THE TRANSIENT RESPONSE OF SPECIES I

A mass balance for species i in pool C_k gives:

$$\text{INLET} - \text{OUTLET} = \text{ACCUMULATION} \tag{2-16}$$

where,

$$\text{INLET} = {}^{k}R\cdot(\text{in}) \tag{2-17}$$

$$\text{OUTLET} = {}^{k}R\cdot{}^{k}F_i \tag{2-18}$$

$$\text{ACCUMULATION} = d^{k}N_i/dt \tag{2-19}$$

Here, t is short for time.

According to the definition 2-8,

$${}^{k}N_i = {}^{k}N\cdot{}^{k}F_i \tag{2-20}$$

Therefore,

$$\text{ACCUMULATION} = d^{k}N\cdot{}^{k}F_i/dt \tag{2-21}$$

or, since ${}^{k}N$ = constant (Section 2.3)

$$\text{ACCUMULATION} = {}^{k}N\cdot d^{k}F_i/dt \tag{2-22}$$

Therefore,

$${}^{k}R\cdot(\text{in}) - {}^{k}R\cdot{}^{k}F_i = {}^{k}N\cdot d^{k}F_i/dt \tag{2-23}$$

or

$$(in) - {}^{k}F_i = \tau_k d{}^{k}F_i/dt \qquad (2\text{-}24)$$

Where,

$$\tau_k = {}^{k}N/{}^{k}R \qquad (2\text{-}25)$$

This is an ordinary differential equation. The solution is:

$${}^{k}F_i = C(t)\cdot e^{-t/\tau_k} \qquad (2\text{-}26)$$

$$C(t) = 1/\tau_k \cdot \int_c^t e^{t/\tau_k}\cdot(in)\cdot dt + C(0) \qquad (2\text{-}27)$$

As can be seen from Eq.2-26, at t=0, ${}^{k}F_i = C(0)$. Thus C(0) cab be determined by the initial condition.

Since we switch from ^{12}CO to ^{13}CO, the initial condition is:

at t = 0,

for $i = k$, ${}^{k}F_i = {}^{k}F_{12}C_k = 1$ (2-28)

for $i \neq k$, ${}^{k}F_i = 0$ (2-29)

Once we know the term (in), we can integrate Eq.2-27 and substitute it into Eq.2-26 to obtain ${}^{k}F_i$.

Appendix A gives a list of (in) forms. The response [illegible] are given in Appendix B.

A computer program (Appendix C) was written to plot the figures for different values of parameters, τ_b, τ_1, τ_2, etc. Figs.2-4 and 2-5 demonstrate the computer simulation for τ_1=20 sec, τb=0.1τ_1, τ_2=0.7τ_1, τ_3=0.7τ_1.

The detailed analysis of pool C_2 and C_3 given in the next two sections requires the knowledge of the term (in) and the switch type (i.e., $^{12}CO \rightarrow {}^{13}CO$ switch or $^{13}CO \rightarrow {}^{12}CO$ switch). For the convenience of the analysis, the term (in) for C_2 and C_3 are denoted as ${}^{k}F_i^0$. The superscript ^{0} reflects the fact that when $\tau_k = 0$, ${}^{k}F_i = (in)$, as can be seen from Eq.2-24.

Eq.2-24 can thus be rewritten as:

$$ {}^{k}F_i^0 - {}^{k}F_i = \tau_k d{}^{k}F_i/dt \qquad (2\text{-}30) $$

We shall utilize this equation in analyzing pool C_2 and C_3.

For pool C_1 and C_b, When we write the transient response of ${}^{13}C_1$ and ${}^{12}C_1$ from pool C_1 and C_b, We will omit the superscript $_1$ for simplicity. In other words, ${}^{1}F_{13}{}_C \equiv {}^{1}F_{13}{}_{C_1}$, and ${}^{b}F_{13}{}_C \equiv {}^{b}F_{13}{}_{C_1}$, etc.

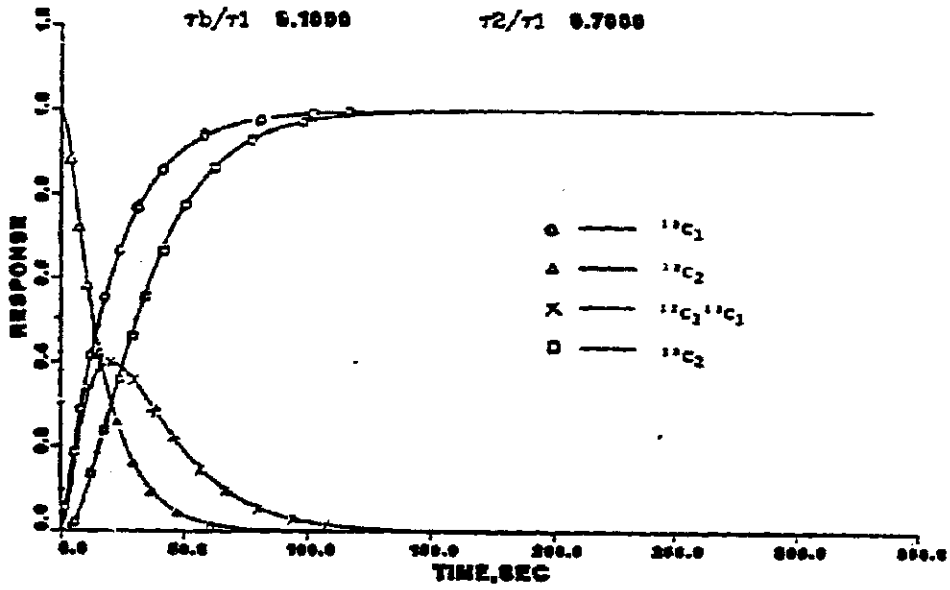

Figure 2-4: A Computer Simulation For Pool C_2

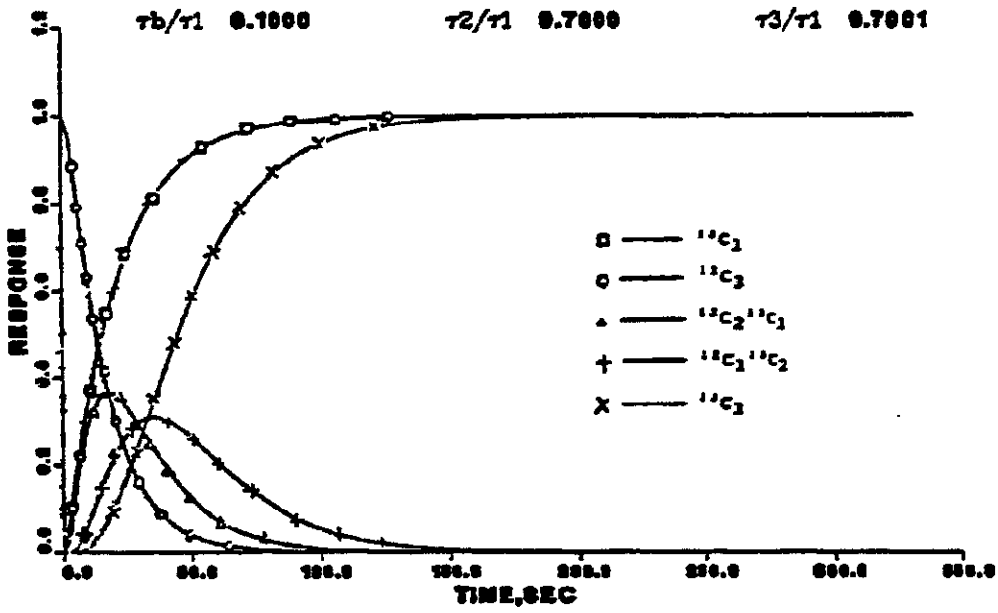

Figure 2-5: A Computer Simulation For Pool C_3

2.5 ANALYSIS OF POOL C_2

The surface CSTR model features as characteristic parameters of the various steps in the surface reaction quantities τ_b, τ_1, τ_2, etc. Among the observables, on the other hand, is the transient ingrowth and decay of $^{13}C_1{}^{12}C_1$. This ingrowth is characterised, among others, by a maximum height (*hm*) and time at a maximum height (*tm*). Now, we attempt to correlate *tm* and *hm* with the parameters τ_b, τ_1 and τ_2 of our model.

When assuming the isotopic constitution of the products leaving the surface to be identical to the isotopic constitution of the products residing at the surface, then the ingrowth curve $^{13}C_1{}^{12}C_1$ reflects the variation of $^2F_{13}C_1{}^{12}C_1$ (defined in Section 2.2.4) with time.

A mass balance on $^{12}C_1{}^{13}C_1$ leads to (c.f.,Section 2.4 and Appendix A):

$$\tau_2 \cdot d^2F_{13}C_1{}^{12}C_1/dt = {}^2F^0_{13}C_1{}^{12}C_1 - {}^2F_{13}C_1{}^{12}C_1 \qquad (2\text{-}31)$$

or,

$$\tau_2 \cdot d^2F_{13}C_1{}^{12}C_1/dt = {}^1F_{13}C \cdot {}^bF_{12}C + {}^1F_{12}C \cdot {}^bF_{13}C - {}^2F_{13}C_1{}^{12}C_1 \qquad (2\text{-}32)$$

where,

$${}^2F^0_{13}C_1{}^{12}C_1 = {}^1F_{13}C \cdot {}^bF_{12}C + {}^1F_{12}C \cdot {}^bF_{13}C \qquad (2\text{-}33)$$

We first consider the limiting case:

$$\tau_2 \equiv 0 \tag{2-34}$$

Substitution of Eq.2-34 into Eq.2-32 yields:

$$0 = {}^{1}F_{13C} \cdot {}^{b}F_{12C} + {}^{1}F_{12C} \cdot {}^{b}F_{13C} - {}^{2}F_{13C_1}{}^{12}C_1 \tag{2-35}$$

or

$${}^{2}F_{13C_1}{}^{12}C_1 = {}^{1}F_{13C} \cdot {}^{b}F_{12C} + {}^{1}F_{12C} \cdot {}^{b}F_{13C} \tag{2-36}$$

Eq.2-36 reflects the fact that in the limit of $\tau_2 = 0$, the isotopic composition within pool C_2, ${}^{2}F_{13C_1}{}^{12}C_1$, follows instantaneously the isotopic composition at the inlet of pool C_2.

Appendix B gives the expressions for ${}^{1}F_{13C}$, ${}^{1}F_{12C}$, ${}^{b}F_{13C}$ and ${}^{b}F_{12C}$. When assuming $\tau_0=0$, we obtain the simplified expressions for ${}^{1}F_{13C}$, ${}^{1}F_{12C}$, ${}^{b}F_{13C}$ and ${}^{b}F_{12C}$ as follows:

$${}^{1}F_{13C} = 1 - \exp(-t/\tau_1) \tag{2-37}$$

$${}^{1}F_{12C} = \exp(-t/\tau_1) \tag{2-38}$$

$${}^{b}F_{13C} = 1 - \exp(-t/\tau_b) \tag{2-39}$$

$${}^{b}F_{12C} = \exp(-t/\tau_b) \tag{2-40}$$

Substituting Eq.2-37 - 2-40 into Eq.2-36, we get:

$$^{2}F^{13}C_1{}^{12}C_1 = f(t/\tau_1,\ \tau b/\tau_1) \qquad (2\text{-}41)$$

or precisely,

$$^{2}F^{13}C_1{}^{12}C_1 = \exp(-t/\tau_1) + \exp(-t/\tau_1 \cdot \tau b/\tau_1) - 2\cdot\exp(-t/\tau_1)\cdot\exp(-t/\tau_1 \cdot \tau b/\tau_1) \qquad (2\text{-}42)$$

When substituting ^{13}CO for ^{12}CO the product will gradually change from $^{12}C_2H_6$ to $^{13}C_2H_6$. The product $^{12}CH_3{}^{13}CH_3$ will only appear in the transition region, i.e., it will first increase and decay thereafter.

Setting:

$$d^{2}F^{13}C_1{}^{12}C_1/dt = 0 \qquad (2\text{-}43)$$

we find that the time at which $^{2}F^{13}C_1{}^{12}C_1$ is the maximum, tm, can be solved from the following implicit function:

$$f(tm/\tau_1,\ \tau b/\tau_1) = 0 \qquad (2\text{-}44)$$

or precisely,

$$\exp(-tm/\tau_1) + \tau_1/\tau b\cdot\exp(-tm/\tau_1\cdot\tau_1/\tau b) = 2\cdot(1 + \tau_1/\tau b)\exp(-tm/\tau_1)\cdot\exp(-tm/\tau_1\cdot\tau_1/\tau b) \qquad (2\text{-}45)$$

Accordingly, $hm = (^{2}F^{13}C_1{}^{12}C_1)_{max}$ can be calculated from Eq.2-42. In general form,

$$hm = f(tm/\tau_1,\ \tau b/\tau_1) \qquad (2\text{-}46)$$

It is readily seen from Eq.2-44 that tm/τ_1 is a function of τ_1 and τ_b:

$$tm/\tau_1 = f(\tau_b/\tau_1) \qquad (2\text{-}47)$$

Combining Eq.2-46 with 2-47, we obtain:

$$hm = f(\tau_b/\tau_1) \qquad (2\text{-}48)$$

Fig.2-6 gives a sketch of relation 2-48, i.e., *hm* versus τ_b/τ_1. As can be seen from this figure, the lowest value of *hm* is 0.5, corresponding to $\tau_b/\tau_1=1$. It is not difficult to give an interpretation of Fig.2-6. For either $\tau_b<<\tau_1$ or $\tau_b>>\tau_1$ we have initially a situation in which one of the two pools (C_1, C_b) has already changed completely to ^{13}C, whereas the other one is still completely ^{12}C. The C_2, which has to be formed by taking one C out of pool C_1 and the other C out of pool C_b, gives almost 100% $^{13}C_1{}^{12}C_1$. Therefore, $^2F_{^{13}C_1{}^{12}C_1}$ tends to unity. On the other hand, when τ_1 equals τ_b ($\tau_b/\tau_1=1$), the isotopic composition of both pools are identical at each point in time (c.f., Eq.2-37 to 2-40) The maximum production of the mixed product $^{12}C_1{}^{13}C_1$ occurs when both reservoirs contain 50% ^{12}C and 50% ^{13}C. In this particular case Eq.2-36 yields

$$^2F_{^{13}C_1{}^{12}C_1} = 0.5\times0.5 + 0.5\times0.5 = 0.5 \qquad (2\text{-}49)$$

We derived above that when $\tau_2 = 0$

hm > 0.5 (c.f. Fig.2-6)

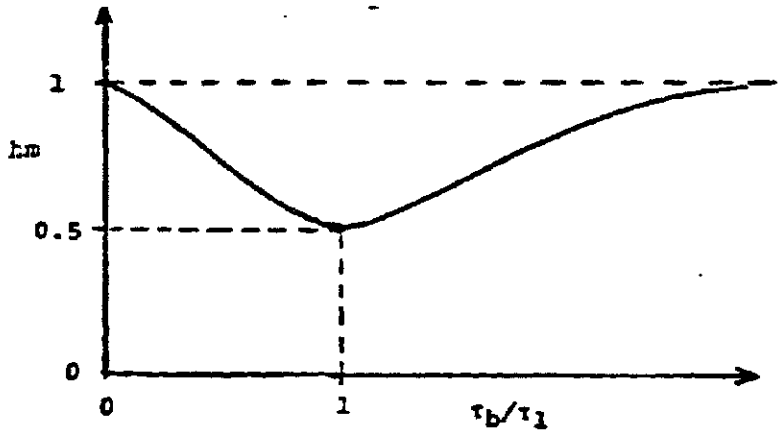

Figure 2-6: *hm* vs τ_b/τ_1 for $\tau_2=0$

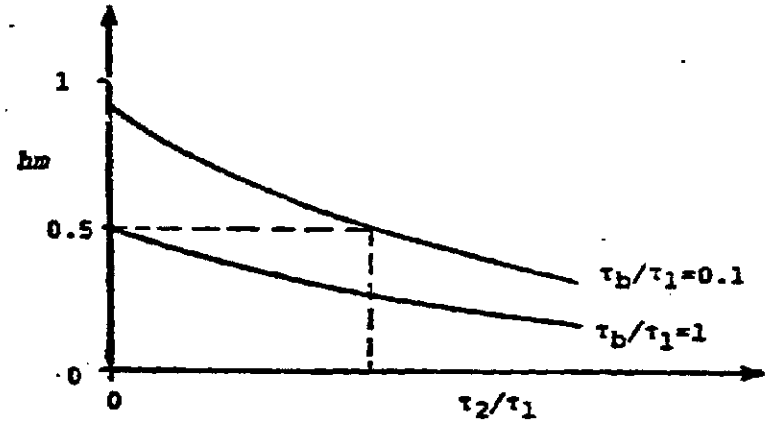

Figure 2-7: *hm* vs τ_2/τ_1

Experiment shows that *hm* < 0.5. Fig.2-6 shows *hm* > 0.5 for $\tau_2/\tau_1 = 0$. According to Fig.2-7, *hm* < 0.5 implies $\tau_2/\tau_1 > 0$.

It will be discussed in Chapter 4 where we invariably observe:

hm < 0.5 (c.f. Fig.4-3, page 57)

We attribute this to the very fact that in our system τ_2 is significantly larger than zero. Whereas the mathematical derivation is given below, we start with an intuitive reasoning.

The input into pool C_2 is being described by Eq.2-36, also in the case that $\tau_2>0$. As discussed earlier, ${}^2F_{13}C_1{}^{12}C_1$ will first increase, then go through a maximum, and subsequently decrease. What we observe in the gas phase is not the input into pool C_2, but the actual composition of pool C_2 (assuming a homogeneous pool C_2). The finite content of pool C_2 (i.e., $\tau_2>0$) will dampen the rise and fall of the input function $({}^1F_{12}C^bF_{13}C + {}^1F_{13}C^bF_{12}C)$ (c.f. Eq.2-32. Therefore, the peak value in ${}^2F_{13}C_1{}^{12}C_1$ will stay below the peak value for $({}^1F_{12}C^bF_{13}C + {}^1F_{13}C^bF_{12}C)$.

Following the mathematical treatment in Section 2.4, we obtain the expression for ${}^2F_{13}C_1{}^{12}C_1$, which is given in Appendix A.

Assuming $\tau_0 = 0$, we get, in a general form,

$${}^2F_{13}C_1{}^{12}C_1=f(t/\tau_1,\ \tau_b/\tau_1,\ \tau_2/\tau_1) \qquad (2\text{-}50)$$

Now, setting,

$$d^2F_{1s}C_1{}^{1s}C_1/dt = 0 \qquad (2\text{-}51)$$

we find,

$$tm/\tau_1 = g(\tau_b/\tau_1,\ \tau_2/\tau_1) \qquad (2\text{-}52)$$

and,

$$hm = g'(\tau_b/\tau_1,\ \tau_2/\tau_1) \qquad (2\text{-}53)$$

In Fig.2-7 we have sketched *hm* vs τ_2/τ_1. It is not difficult to have an interpretation of Fig.2-7.

Setting τ_1 = constant, and τ_b/τ_1 = constant,

For the rising period of $^2F_{1s}C_1{}^{1s}C_1$, i.e., $0 < t < tm$,

$$d^2F_{1s}C_1{}^{1s}C_1/dt > 0 \qquad (2\text{-}54)$$

Thus, Eq.2-31 becomes:

$$^2F^0_{1s}C_1{}^{1s}C_1 - {}^2F_{1s}C_1{}^{1s}C_1 > 0 \qquad (2\text{-}55)$$

or

$$^2F_{1s}C_1{}^{1s}C_1 < {}^2F^0_{1s}C_1{}^{1s}C_1 \qquad (2\text{-}56)$$

When $^2F_{1s}C_1{}^{1s}C_1$ reaches its maximum, i.e., $t = tm$.

$$d^2F_{1s}C_1{}^{1s}C_1/dt = 0 \qquad (2\text{-}57)$$

or

$$^2F_{1s}C_1{}^{1s}C_1 = {}^2F^0_{1s}C_1{}^{1s}C_1 \qquad (2\text{-}$$

or,

$$hm = {}^{2}F^{\hat{}}{}_{3}C_{1}{}^{1}{}_{2}C_{1} \tag{2-59}$$

For the decreasing period of ${}^{2}F_{1}{}_{2}C_{1}{}^{1}{}_{3}C_{1}$, i.e., $t > tm$,

$$d^{2}F_{1}{}_{3}C_{1}{}^{1}{}_{2}C_{1}/dt < 0 \tag{2-60}$$

Thus,

$${}^{2}F_{1}{}_{3}C_{1}{}^{1}{}_{2}C_{1} > {}^{2}F^{\hat{}}{}_{3}C_{1}{}^{1}{}_{2}C_{1} \tag{2-61}$$

Combining Eq.2-56, 2-58 and 2-61 with the boundary conditions (${}^{2}F_{1}{}_{3}C_{1}{}^{1}{}_{2}C_{1} = 0$ and ${}^{2}F^{\hat{}}{}_{3}C_{1}{}^{1}{}_{2}C_{1} = 0$ at $t = 0$ and ∞), we can sketch Fig.2-8. It is readily seen that the maximum of ${}^{2}F^{\hat{}}{}_{3}C_{1}{}^{1}{}_{2}C_{1}$ ($h\hat{m}$) is at $0 < t < \hat{tm}$. In other words, ${}^{2}F^{\hat{}}{}_{3}C_{1}{}^{1}{}_{2}C_{1}$ must peak before ${}^{2}F_{1}{}_{3}C_{1}{}^{1}{}_{2}C_{1}$, which, combined with Eq.2-59, implies that

$$hm < h\hat{m} \tag{2-62}$$

It is seen from Fig.2-7 that for fixed τ_b/τ_1, *hm* decreases monotoneously with incresing τ_2/τ_1. Values well below 0.5 can be obtained for $\tau_2>0$. We will utilize those results in Chapter 4 to estimate τ_2 for the systems actually studied.

We now turn our attention to the location of *hm* in the time domain.

When $\tau_2=0$, we have:

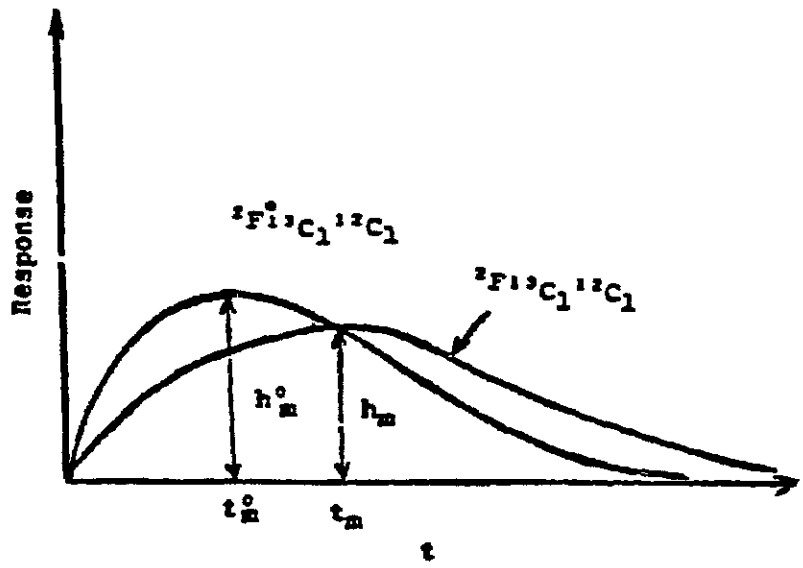

Figure 2-8: The relation between hm, hm̂, tm and tm̂

$tm/\tau_1 = f(\tau_b/\tau_1)$ (c.f., Eq.2-47)

A plot of tm/τ_1 vs $\tau b/\tau_1$ is shown in Fig.2-9. It is drawn as follows:

Setting τ_1 = constant, when $\tau_b/\tau_1 = 0$, ${}^{b}F_{12}C = 0$, ${}^{b}F_{13}C = 1$. Eq.2-36 becomes:

$$ {}^{2}F_{12}C_1{}^{13}C_1 = {}^{1}F_{12}C \qquad (2\text{-}63) $$

Therefore,

$hm = 1$, at $tm/\tau_1 = 0$.

When $\tau_b/\tau_1 = \infty$, ${}^{b}F_{12}C = 1$, ${}^{b}F_{13}C = 0$. Eq.2-36 becomes:

$$ {}^{2}F_{12}C_1{}^{13}C_1 = {}^{1}F_{13}C \qquad (2\text{-}64) $$

Therefore,

$hm = 1$, at $tm/\tau_1 = \infty$.

When $\tau_b/\tau_1 = 1$, ${}^{b}F_{12}C = {}^{1}F_{12}C$, and ${}^{b}F_{13}C = {}^{1}F_{13}C$. Eq.2-36 becomes:

$$ {}^{2}F_{12}C_1{}^{13}C_1 = 2\cdot{}^{1}F_{12}C\cdot{}^{1}F_{13}C \qquad (2\text{-}65) $$

Setting $\tau_b/\tau_1 = 1$ in Eq.2-45, tm/τ_1 can be solved to yield an analytical solution:

$$ tm/\tau_1 = \ln 2. \qquad (2\text{-}66) $$

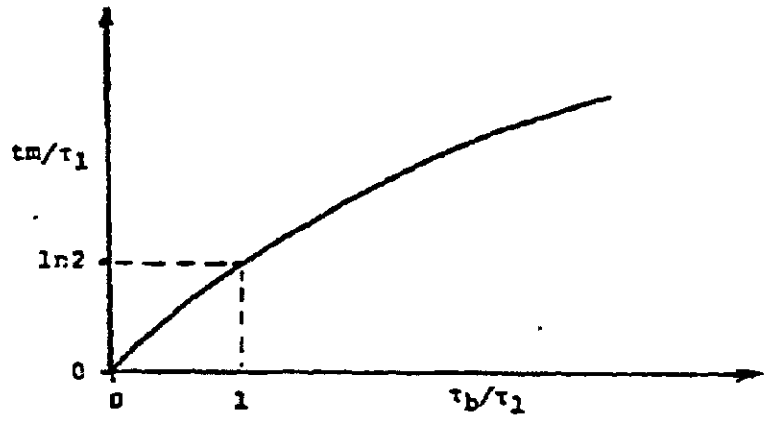

Figure 2-9: tm/τ_1 vs τ_b/τ_1 for $\tau_2=0$

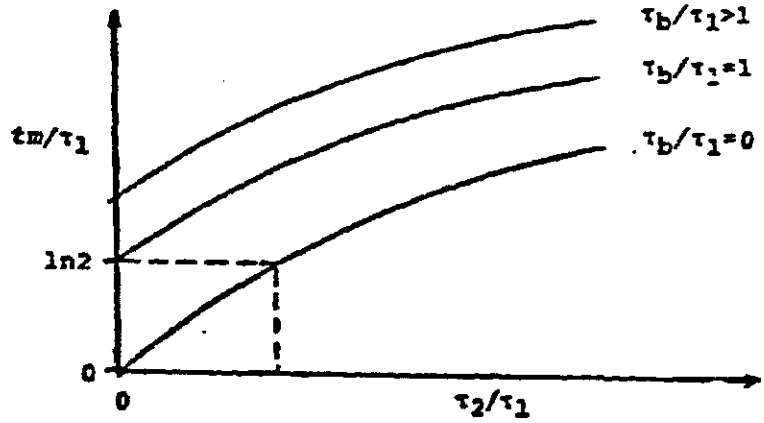

Figure 2-10: tm/τ_1 vs τ_2/τ_1

Experiment shows that $tm = t1 = \tau_1 \times \ln 2$. Fig.2-10 tells us that since $\tau_2/\tau_1 > 0$ (from Fig.2-6 and 2-7) only $\tau_b/\tau_1 < 1$ can result in the case $tm=t1$.

Substituting Eq.2-66 into 2-42 yields:

$hm = 0.5$

Fig.2-6 and 2-9 were sketched Based on hm's and tm's at these three different values of τ_b/τ_1 :0, 1, ∞. As can be seen from Fig.2-9, tm/τ_1 increases with increasing τ_b/τ_1.

In Fig.2-9, we observe that when $\tau_1=\tau_b$, ${}^2F_{1\,3}C_1{}^{1\,2}C_1$ peaks at ${}^1F_{1\,3}C_1={}^bF_{1\,3}C_1=0.5$, i.e., at $t1=\tau_1 \times \ln 2$. Therefore, the abscissa $\tau_b/\tau_1=1$ in Fig.2-9 corresponds to the ordinate $t1=\tau_1 \times \ln 2$. It follows that

$$tm < t1, \quad \text{at } \tau_b/\tau_1 < 1;\ \tau_2 = 0 \tag{2-67}$$

and,

$$tm > t1, \quad \text{at } \tau_b/\tau_1 > 1;\ \tau_2 = 0 \tag{2-68}$$

Next we consider the effect of $\tau_2>0$ on tm.

It can be verified from Eq.2-50 and 2-51 that,

$$tm/\tau_1 = g(\tau_b/\tau_1,\ \tau_2/\tau_1) \tag{2-69}$$

In Fig.2-10, we have plotted tm/τ_1 versus τ_2. From Fig.2-8 we know that ${}^2F_{1\,2}C_1{}^{1\,3}C_1$ must peak before ${}^2F_{1\,2}C_1{}^{1\,3}C_1$, naturally, at the same τ_b/τ_1. In other words,

$$tm < tm \tag{2-70}$$

(for the same τ_b/τ_1)

Here, $\hat{tm}$ is the tm at $\tau_2 = 0$.

It is apparent that at fixed values for τ_b/τ_1, tm/τ_1 increases monotoneously with τ_2/τ_1.

This can be fully understood when viewing pool C_2 as an element which dampens the input function (${}^1F_{12_C}{}^bF_{13_C}$ + ${}^1F_{13_C}{}^bF_{12_C}$) with dampening constant τ_2: with increasing τ_2 the peak values is dampened and shifted towards longer time.

It can be seen from Fig.2-10 that for a $\tau_b/\tau_1 > 1$, tm/τ_1 will be always larger than $t1/\tau_1$ (= ln 2) for $\tau_2/\tau_1 > 0$, whereas for $\tau_b/\tau_1 < 1$, a sufficient large τ_2/τ_1 can make $tm/\tau_1 = t1/\tau_1$. Here, t1 is defined as the time at which ${}^1F_{13_C} = {}^1F_{12_C} = 0.5$.

We will utilize the above results to interpret what is being observed in practice.

2.6 ANALYSIS OF POOL C_3

The task in this part is to characterize pool C_3 in terms of some physically measureable quantities. Unlike the previous analysis, the following discussion will not analyze the ingrowth of the compounds containing both ^{13}C and ^{12}C, i.e., $^{13}C_1{}^{12}C_2$ and $^{13}C_2{}^{12}C_1$ Because it is difficult to do that. A simple mass balance treatment is given below.

Although all transient responses from pool C_3 reflec-

the characteristics of pool C_3, only the simplest possible relation is desired. Below, we will give some intuitive reasons why we chose the present treatment to characterize pool C_3.

First, in our experiment, we observe that ($F^{13}C$ in C_3) - ($F^{13}C$ in C_2) ≈ ($F^{13}C$ in C_2) - ($^1F^{13}C$). Therefore, at a glance, one may readily envisage that if the desired relation for judging whether τ_3 is observable contains ($F^{13}C$ in C_3), ($F^{13}C$ in C_2) and $^1F^{13}C$, it may reflect characteristics of pool C_3 with a simple form.

Secondly, $^bF^{13}C$ is not physically measureable. Therefore, we shall omit this term in the desired relation. Since C_b-* is added to the C_k-* for chain growth, the mass balance on C_{k+1} alone, on the one hand, is not enough to cancel the term $^bF^{13}C$. On the other hand, because C_b-* is added into C_k-*, one would imagine that the mathematical formula would not be too complex, leaving a chance to cancel $^bF^{13}C$ by combining expressions for two consecutive pools. This is what we will actually do in this work.

Thirdly, if we make mass balances on a pool, (Fig.2-11), we have to deal directly with the pool itself, which will makes the analysis complex. Now, let us consider points A and B. The inlets entering A (or B) are purely C_1-* (or C_2-*) and C_b-*. There is no accumulation at point A (or B). In fact, it is just for this "non-accumulation" feature that we choose point A instead of pool C3 to perform mass balances.

Before presenting the detailed analysis, we shall give the final expression below:

If $3\cdot(F^{13}C \text{ in } C_2 - F^{13}C \text{ in } C_3) > {}^{1}F^{13}C - F^{13}C \text{in} C_2$

then τ_3 is observable. (2-71)

Now, consider Fig.2-11. We shall make mass balances on the crossing points A and B, respectively.

First of all, the input of C_1 to point A must be equal to the input of C_b to point A. The reason is that, to form a C_2, one carbon shall be from C_1 and another carbon shall be from C_b. They have to react with each other. In other words, if in one second, ${}^{2}R$ of C_2 is formed, that will require ${}^{2}R$ of C_1 and ${}^{2}R$ of C_b.

We shall write the mass balance on atom basis, i.e., make a mass balance on the total carbon numbers on point A:

$$C \text{ in } C_2 = C \text{ in } C_1 + C \text{ in } C_b \qquad (2\text{-}72)$$

Now,

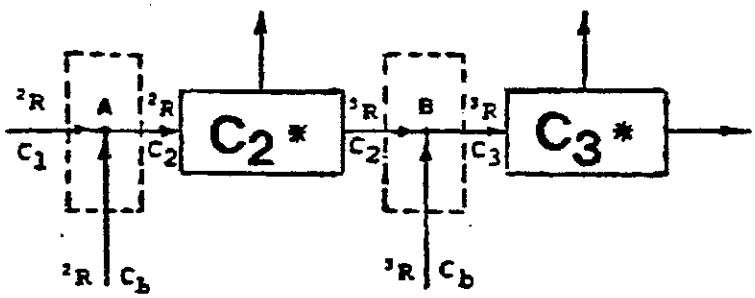

Figure 2-11: Mass Balance on C_2 and C_3

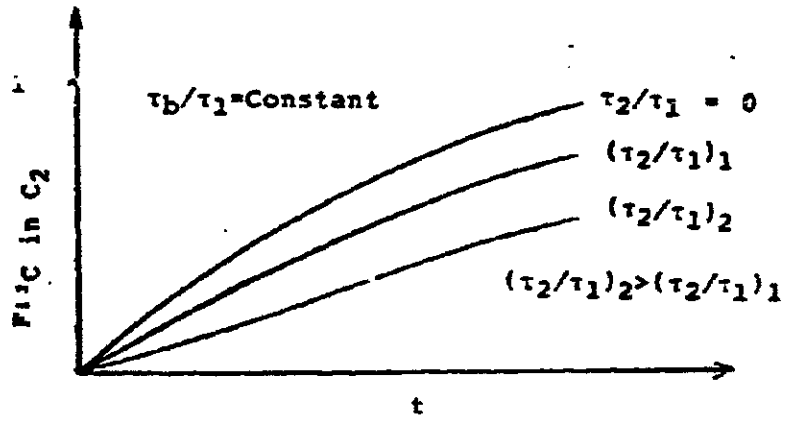

Figure 2-12: $F^{13}C$ in C_2 vs t

$$C \text{ in } C_2 = 2x^2R \tag{2-73}$$

$$C \text{ in } C_1 = {}^2R \tag{2-74}$$

$$C \text{ in } C_b = {}^2R \tag{2-75}$$

therefore,

$$2x^2R = 1x^2R + 1x^2R \tag{2-76}$$

Next, a mass balance is made for ^{13}C, still on point A,

$$^{13}C \text{ in } C_2 = {}^{13}C \text{ in } C_1 + {}^{13}C \text{ in } C_b \tag{2-77}$$

Now,

$$^{13}C \text{ in } C_2 = (C \text{ in } C_2)\times(\text{fraction of } {}^{13}C)$$

$$= 2 \cdot {}^2R \cdot F^{0}_{{}^{13}C \text{ in } C_2} \tag{2-78}$$

$$^{13}C \text{ in } C_1 = (C \text{ in } C_1)\times(\text{fraction of } {}^{13}C)$$

$$= {}^2R \cdot F_{{}^{13}C \text{ in } C_1} = {}^2R \cdot {}^1F_{{}^{13}C} \tag{2-79}$$

$$^{13}C \text{ in } C_b = (C \text{ in } C_b)\times(\text{fraction of } {}^{13}C)$$

$$= {}^2R \cdot {}^bF_{{}^{13}C} \tag{2-80}$$

In Eq.2-78, a superscript ^{0} is used to represent the inlet to pool C_2 (c.f., Section 2.4).

Substituting Eq.2-78 ~ 2-80 into Eq.2-77 yields:

$$2 \cdot {}^{2}R \cdot F^{\circ}{}^{13}C \text{ in } C_2 = {}^{2}R \cdot {}^{1}F^{13}C + {}^{2}R \cdot {}^{b}F^{13}C \qquad (2\text{-}81)$$

Cancelling ^{2}R, we get,

$$2 \cdot F^{\circ}{}^{13}C \text{ in } C_2 = {}^{1}F^{13}C + {}^{b}F^{13}C \qquad (2\text{-}82)$$

or

$$F^{\circ}{}^{13}C \text{ in } C_2 = 1/2({}^{1}F^{13}C + {}^{b}F^{13}C) \qquad (2\text{-}83)$$

A mass balance for ^{13}C in C_2 on pool C_2 pool leads to (c.f., Section 2.4):

$$F^{\circ}{}^{13}C \text{ in } C_2 - F^{13}C \text{ in } C_2 = \tau_2 \cdot dF^{13}C \text{ in } C_2/dt \qquad (2\text{-}84)$$

Since we switch from ^{12}CO to ^{13}CO,

$$dF^{13}C \text{ in } C_2/dt > 0 \qquad (2\text{-}85)$$

Therefore, for $\tau_2 > 0$,

$$F^{13}C \text{ in } C_2 < F^{\circ}{}^{13}C \text{ in } C_2 \qquad (2\text{-}86)$$

Fig.2-12 is the plot of $F^{13}C$ in C_2 vs τ_2/τ_1. It is readily seen that the term $F^{13}C$ in C_2 is delayed by pool C_2. The greater is the τ_2, the smaller the $F^{13}C$ in C_2 at a given time.

or, with Eq.2-83 and 2-86, we obtain,

$$F^{13}C \text{ in } C_2 < 1/2({}^{1}F^{13}C + {}^{b}F^{13}C) \quad (2\text{-}87)$$

i.e.,

$$2 \cdot F^{13}C \text{ in } C_2 - {}^{1}F^{13}C < {}^{b}F^{13}C \quad (2\text{-}88)$$

Next, we shall make mass balances at point B.

First of all, for the total carbon,

$$\text{Outlet} = {}^{3}R = \text{the rate of } C_3 \quad (2\text{-}89)$$

$$\text{Inlet of } C_2 = {}^{3}R \quad (2\text{-}90)$$

$$\text{Inlet of } C_1^b = {}^{3}R \quad (2\text{-}91)$$

On atom basis,

$$C \text{ in } C_3 = C \text{ in } C_2 + C \text{ in } C_b \quad (2\text{-}92)$$

Now,

$$C \text{ in } C_3 = 3 \cdot {}^{3}R \quad (2\text{-}93)$$

$$C \text{ in } C_2 = 2 \cdot {}^{3}R \quad (2\text{-}94)$$

$$C \text{ in } C_b = 1 \cdot {}^{3}R \quad (2\text{-}95)$$

A mass balance on ^{13}C leads to,

$$^{13}C \text{ in } C_3 = {}^{13}C \text{ in } C_2 + {}^{13}C \text{ in } C_b \quad (2\text{-}96)$$

Where,

$$^{13}C \text{ in } C_3 = 3 \cdot {}^{3}R \cdot F^{\circ}{}_{13}C \text{ in } C_3 \qquad (2\text{-}97)$$

$$^{13}C \text{ in } C_2 = 2 \cdot {}^{3}R \cdot F_{13}C \text{ in } C_2 \qquad (2\text{-}98)$$

$$^{13}C \text{ in } C_b = 1 \cdot {}^{3}R \cdot {}^{b}F_{13}C \qquad (\text{c.f. Eq.2-80})$$

Substituting the above equations into Eq.2-96,

$$3 \cdot F^{\circ}{}_{13}C \text{ in } C_3 = 2 \cdot F_{13}C \text{ in } C_2 + F_{13}C \text{ in } C_b \qquad (2\text{-}99)$$

or

$$3 \cdot F^{\circ}{}_{13}C \text{ in } C_3 - 2 \cdot F_{13}C \text{ in } C_2 = {}^{b}F_{13}C \qquad (2\text{-}100)$$

Comparing Eq.2-100 and Eq.2-88, we obtain:

$$2 \cdot F_{13}C \text{ in } C_2 - {}^{1}F_{13}C < 3 \cdot F^{\circ}{}_{13}C \text{ in } C_3 - 2 \cdot F_{13}C \text{ in } C_2 \qquad (2\text{-}101)$$

or

$$3 \cdot (F_{13}C \text{ in } C_2 - F^{\circ}{}_{13}C \text{ in } C_3) < {}^{1}F_{13}C - F_{13}C \text{ in } C_2 \qquad (2\text{-}102)$$

We now write the mass balance on pool C_3 for ^{13}C in C_3 (c.f., Section 2.4):

$$F^{\circ}{}_{13}C \text{ in } C_3 - F_{13}C \text{ in } C_3 = \tau_3 \cdot dF_{13}C \text{ in } C_3/dt \qquad (2\text{-}103)$$

When $\tau_3 = 0$

$$F^{\circ}{}_{13}C \text{ in } C_3 - F_{13}C \text{ in } C_3 = 0 \qquad (2\text{-}104)$$

or

$$F^{\circ}{}_{13}C \text{ in } C_3 = F_{13}C \text{ in } C_3 \qquad (2\text{-}105)$$

Substituting Eq.2-105 into 2-102 yields,

$$3\cdot(F^{13}C \text{ in } C_2 - F^{13}C \text{ in } C_3) < {}^{1}F^{13}C - F^{13}C \text{ in } C_2 \quad (2\text{-}106)$$

Eq.2-105 and 2-106 reflect the fact that in the limit of $\tau_3 = 0$, the isotopic composition within pool C_3, $F^{13}C$ in C_3, follows instantaneously the isotopic composition at the inlet of pool C_3, and $3\cdot(F^{13}C \text{ in } C_2 - F^{13}C \text{ in } C_3)$ is less than $(F^{13}C \text{ in } C_1 - F^{13}C \text{ in } C_2)$.

Although Eq.2-106 does not agree with the experimental result (c.f., Fig.4-5, page 59), it gives us a hint: whether τ_3 is observable may be reflected in the relation between $3\cdot(F^{13}C \text{ in } C_2 - F^{13}C \text{ in } C_3)$ and $(F^{13}C \text{ in } C_1 - F^{13}C \text{ in } C_2)$.

We now consider the case where $\tau_3 > 0$.

When switching from ^{12}CO to ^{13}CO,

$$dF^{13}C \text{ in } C_3/dt > 0 \quad (2\text{-}107)$$

Substituting Eq.2-107 into Eq.2-103, we obtain,

$$F^{\hat{1}3}C \text{ in } C_3 - F^{13}C \text{ in } C_3 > 0 \quad (2\text{-}108)$$

or

$$F^{\hat{1}3}C \text{ in } C_3 > F^{13}C \text{ in } C_3 \quad (2\text{-}109)$$

Because of pool C_3, the outlet $F^{13}C$ in C_3 is less than $F^{13}C$ in C_3 at any time (See Fig.2-13). The larger the ...

the smaller the $F^{13}C$ in C_3. Therefore, If τ_3 is significantly large, $F^{13}C$ in C_3 will be much less than $F^{13}C$ in C_3, see Fig.2-13. This will lead to a larger difference between $F^{13}C$ in C_2 and $F^{13}C$ in C_3, which in turn may be greater than one-third of the difference between $^1F^{13}C$ and $F^{13}C$ in C_2. Fig.2-14 shows this situation.

Setting,

$$\delta \equiv 3\cdot(F^{13}C \text{ in } C_2 - F^{13}C \text{ in } C_3) - (^1F^{13}C - F^{13}C \text{ in } C_2) \qquad (2\text{-}110)$$

it is easily seen from Fig.2-14 that under the shaded area, although τ_3/τ_1 is larger than zero, δ is less than zero. in this case, one cannot tell whether τ_3 is observable. above the shaded area, δ is greater than zero. Therefore, τ_3 can be surely observed.

We shall summarize the result from the above analysis:

If $3\cdot(F^{13}CinC_2 - F^{13}CinC_3) > {}^1F^{13}C - F^{13}CinC_2$

then τ_3 is observable. (2-111)

This results will be utilized in Chapter 4 to interpret our observations.

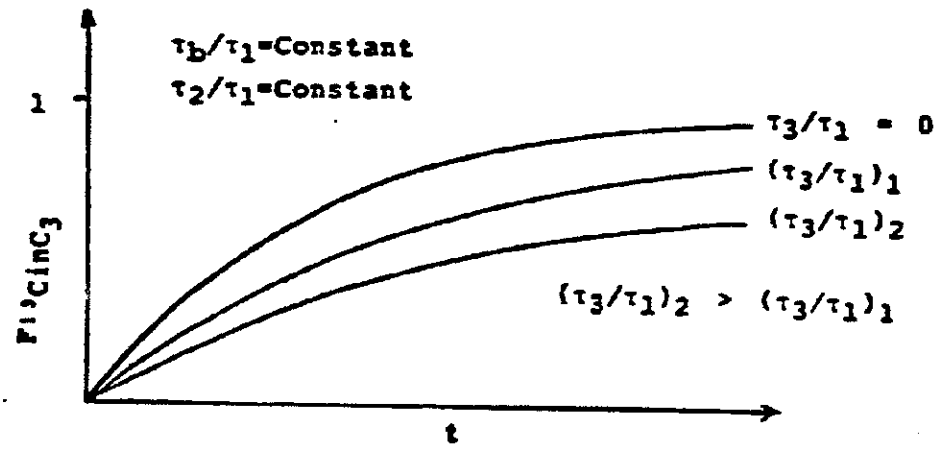

Figure 2-13: $F^{13}CinC_3$ vs t

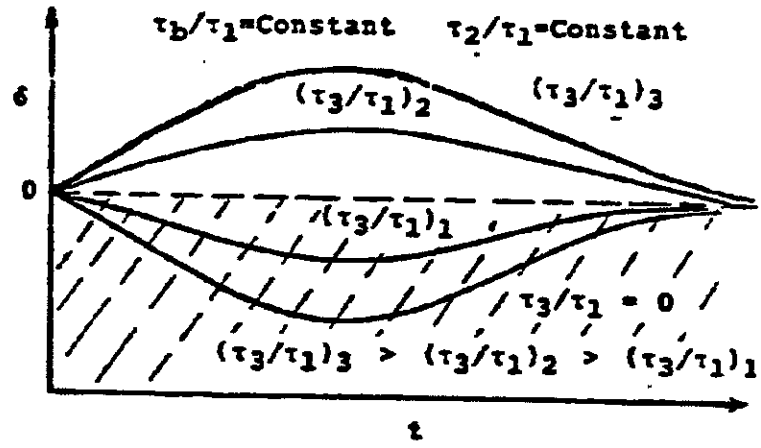

Figure 2-14: δ vs t

This is an imaginary plot: (1) at t = 0, $^1F^{13}C$ = 0, $F^{13}C$ in C_2 = 0, $F^{13}C$ in C_3 = 0. Therefore, δ = 0. (2) at t = ∞, $^1F^{13}C$ = 1, $F^{13}C$ in C_2 = 1, $F^{13}C$ in C_3 = 1. Therefore, δ = 0. (3) at 0 < t < ∞, depending on τ_3/τ_1, δ will be greater than, equal to, or less than